# Immiscible Ethylene Vinyl Acetate and Nylon Blends Processed Below Nylon Melting Temperature

A. TZUR,[1] M. NARKIS,[1] A. SIEGMANN[2]

[1] Department of Chemical Engineering, Technion, Israel Institute of Technology, Haifa 32000, Israel

[2] Department of Materials Engineering, Technion, Israel Institute of Technology, Haifa 32000, Israel

**ABSTRACT:** This article focuses on unique compounding and processing conditions at a temperature slightly below the melting temperature of the dispersed phase and well above the melting peak temperature of the matrix. Compounding and processing were carried out at the same temperature. Fibrillar morphologies were obtained by blending ethylene vinyl acetate (EVA) copolymer with nylon 6 (N6) and compounding and processing them slightly below the N6 melting temperature. A hot, soft-solid particle drawing mechanism that operates in such processing conditions caused fibrillation of the N6 particles and formation of highly oriented fibril-filled composites throughout the entire volume. Morphological observations were made in the core region. Enhancement of some mechanical properties and interesting morphological structures were found in some of the blends. The melt elasticity, which was measured by the die swell of the filaments, was maximum at a temperature slightly below the N6 melting temperature, which supported the concept of fibrillation by processing it slightly below the melting temperature of the dispersed phase. © 2001 John Wiley & Sons, Inc. J Appl Polym Sci 82: 661–671, 2001

**Key words:** immiscible blends; ethylene vinyl acetate; nylon 6; melting temperature

## INTRODUCTION

Immiscible polymer blends form multiphase systems with a minor phase morphology such as spheres, ellipsoids, fibrils, platelets, and ribbons.[1] Structuring of immiscible polymer blends through deformation and orientation of the dispersed domains is a result of the flow fields experienced in melt processing. During shear and elongational flow, dispersed spherical droplets can form fibrillar domains oriented along the flow direction.[2] The major parameters that affect fibril formation include the blend composition and the viscosity ratio of the dispersed to the continuous phase.[3] For viscosity ratios less than or equal to unity, melt droplets are elongated during flow and form fibrils oriented in the flow direction. However, when the dispersed phase exhibits a higher viscosity, only very high stress levels are able to deform the suspended droplets. Alle and Lyngaae-Jorgensen[4] proposed that for a dispersed phase of lower viscosity than the matrix, these fibrils tend to break up and "recoil." However, for a higher viscosity dispersed phase the fibrillar morphology was stable. It is well established that elongational flow is more efficient than shear flow in deforming the dispersed phase.[5] Following these principles, Kamal and coworkers[6] utilized controlled processing conditions to attain a laminar morphology in polypropylene/ethylene vi-

nyl (EV) hydroxide and high-density polyethylene (HDPE)/nylon 6 (N6) blends. The laminar morphology in blow-molded containers was developed by extruding HDPE/N6 blends under special conditions.[7–9]

Van Oene[10] and Elmendorp[11] investigated the effect of additional parameters (melt elasticity and normal stresses) on the phase morphology of polymer blends. Van Oene proposed that normal stresses can imbalance the interfacial energy over the interface in the melt state and determine the shape of the dispersed phase.[10] Elmendorp showed that viscoelasticity enhances the droplet stability.[11] Blends of HDPE/N6 were melt mixed at 250°C[12–17] and showed highly elongated N6 particles as ribbons extruded at different draw ratios. Utracki et al.[15] measured the steady-state and dynamic flow properties of HDPE/N6 blends (melt mixed at 250°C) at 150, 200, and 250°C. [The N6 melt temperature ($T_m$) is 220°C.] The rheological behavior was discussed in terms of the morphology. The influence of the N6 content on the steady-state shear viscosity is temperature dependent.[14] At 150°C the dispersed N6 phase acted as a solid filler, causing an increase in the viscosity with content. At 250°C the low viscosity N6 melt migrated to the wall, causing a viscosity reduction with content. At 200°C these two effects were nearly compensated, resulting in a viscosity that was practically independent of the content. Stress-induced fibrillation was observed at all processing temperatures, where the operating mechanism was clearly extensional.

Polypropylene and N6 were extruded at 230°C,[18] and then the granules were rolled in a twin-roll milling machine at 170°C and compression molded at 180°C. Morphology studies showed that the fibrillation of N6 had already occurred in the metering zone rather than in the die. The fibrillar structure was preserved even at slow cooling rates.

Addonizio et al.[19] studied blends of N6 with an EV acetate copolymer (EVA) extruded at 260°C. The mode and the state of dispersion of the minor component were found to be controlled by the composition and extrusion temperature. At 220°C the N6 domains in a 60EVA/40N6 blend were elongated along the extrusion direction, forming irregular N6 rods in the outer regions and spherical particles toward the center.

The properties and morphology of injection-molded blends of N6 and EVA copolymers with different VA contents were also investigated.[20] Scanning electron microscopy (SEM) analysis showed that processing induced an inhomogeneous distribution of the dispersed phase with a skin layer almost free of the minor component and an increasing copolymer concentration in the specimen's core.

The objective of the present study was to investigate the morphology of EVA/N6 blends, which were processed slightly below the melting temperature of the dispersed N6 phase. At such processing temperatures the dispersed nylon particles are expected to behave as deformable soft elastic particles. Thus, the compounding and processing steps were both performed at temperatures well above the EVA melting temperature and slightly below the N6 melting temperature.

$$T_{m,\text{EVA}} \ll T_{\text{compounding}} = T_{\text{processing}} < T_{m,\text{Ny-6}}$$

Studies with such compounding–processing conditions were not found in the literature. Reference systems were also produced under ordinary blending and processing conditions, which is at a temperature above the melting of both polymers.

## EXPERIMENTAL

### Materials

The polymers used in this study were a Reablene EV copolymer containing 19% VA and two grades of N6, which were Capron 8200 HS (medium viscosity, Allied Signal) and Polyram PN60 LS9 (low viscosity, Polyram). In some experiments a highly structured, electrically conductive carbon black (CB, Ketjenblack EC-300, Akzo) was added.

### Blending and Processing

The N6 pellets were ground in a Wiley mill using a 2-mm screen and subsequently dry blended with the EVA granules. The 70EVA/30N6 mixtures were dried (80°C overnight under a vacuum) prior to compounding and processing. An Arburg injection-molding machine or a Brabender twin-screw extruder were used to compound the EVA/N6 mixtures. Following granulation, the blends were processed by injection molding into a standard ASTM mold maintained at 40°C, or filaments were produced by a Thoret single-screw extruder. The compounding and processing temperatures for the EVA/N6 blends were identical:

190, 205, 210, 215, 220, or 240°C ($T_{m,\text{N6}}$ = 219°C). A concentrate of 6 wt % CB in EVA was prepared in a Brabender twin-screw extruder and added to some EVA/N6 mixtures before compounding at 210°C in order to study the effect of CB on the morphology that was obtained. A future study will focus on the electrical behavior of such systems.

### Characterization

The thermal behavior was determined using a Mettler TA3000 machine with a DSC-30 module. The melt viscosity of the neat polymers was determined at 240°C using an Instron capillary rheometer equipped with a 5.08 × 0.127 cm (2 ×0.05 in.) capillary (*L/D* = 40). Tensile tests were carried out using an Instron 5568 universal testing machine at a crosshead speed of 5 cm/min (10-cm gauge length). Specimens were injection molded (ASTM D638) or extruded (Thoret single-screw extruder) to produce filaments of circular cross section.

The blend phase morphology was studied using a Jeol 5400 SEM microscope. The injection-molded bars and the extruded filaments were fractured at liquid nitrogen temperature at an angle close to parallel to the flow direction, and they were subsequently sputtered with gold. The dynamic mechanical thermal analysis (DMTA) of the properties of selected compositions was performed using a Perkin–Elmer Series 7 DMTA instrument in three-point bending mode and operated at 1 Hz under a nitrogen atmosphere at a
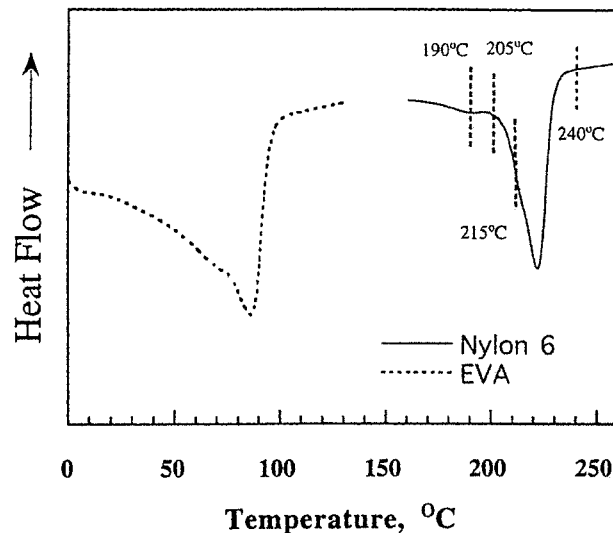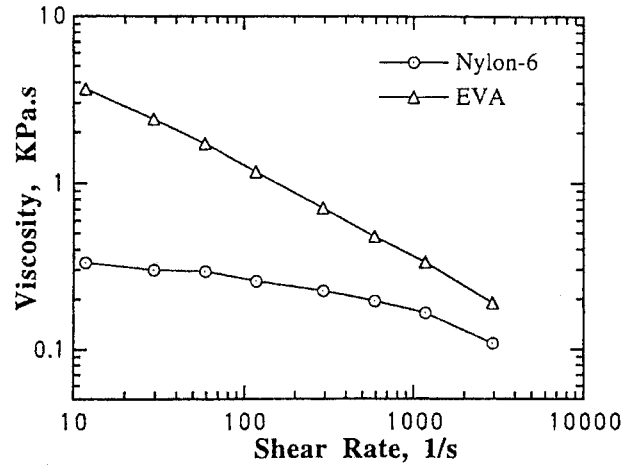


**Figure 2** The viscosity versus the shear rate of EVA and N6 at 240°C.

heating rate of 2°C/min. Experiments were conducted using the DMTA instrument in the creep mode to produce stress–strain curves for the different blends, along with the creep compliance. These experiments were performed in three-point bending mode on samples from the injection-molded specimens that were cut transverse and parallel to the flow direction.

## RESULTS AND DISCUSSION

The processing temperatures marked on the N6 thermogram (Fig. 1) were below and above the polymer melting peak temperature (219°C). Processing below 219°C caused the blends to behave
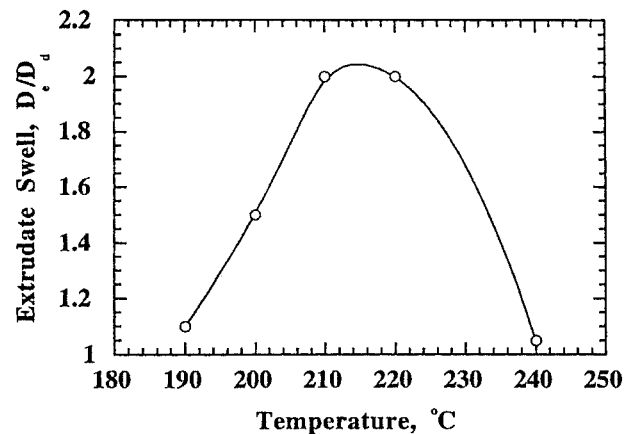


**Figure 1** DSC thermograms of EVA and N6.



**Figure 3** The extrudate swell ratio ($D_e/D_d$) versus the extrusion temperature of the 70EVA/30N6 blend ($D_e$, extrudate diameter; $D_d$, die diameter).
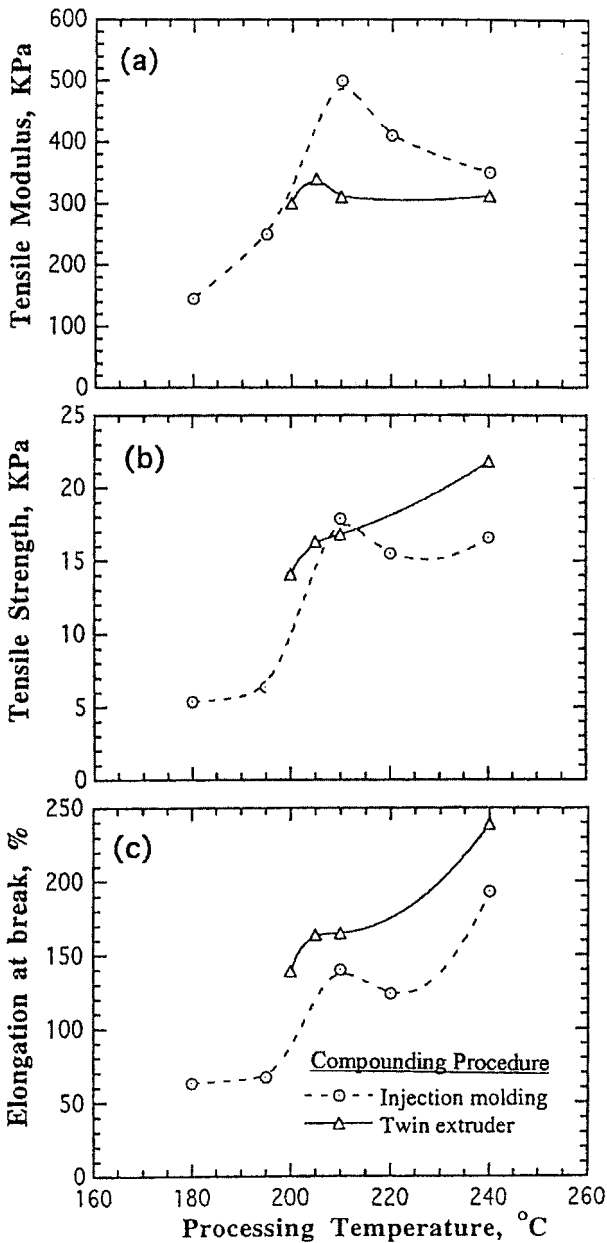
as polymer composites filled with soft-solid deformable particles. At a processing temperature of 240°C there was regular immiscible blend behavior. The original size of the ground N6 particles was found to have an important effect on the fibril formation.

## Rheology

The apparent viscosity of the EVA and N6 (Capron) at 240°C is shown in Figure 2. Both polymers exhibited pseudoplastic behavior, EVA more so than N6. At the lower shear rates the EVA had
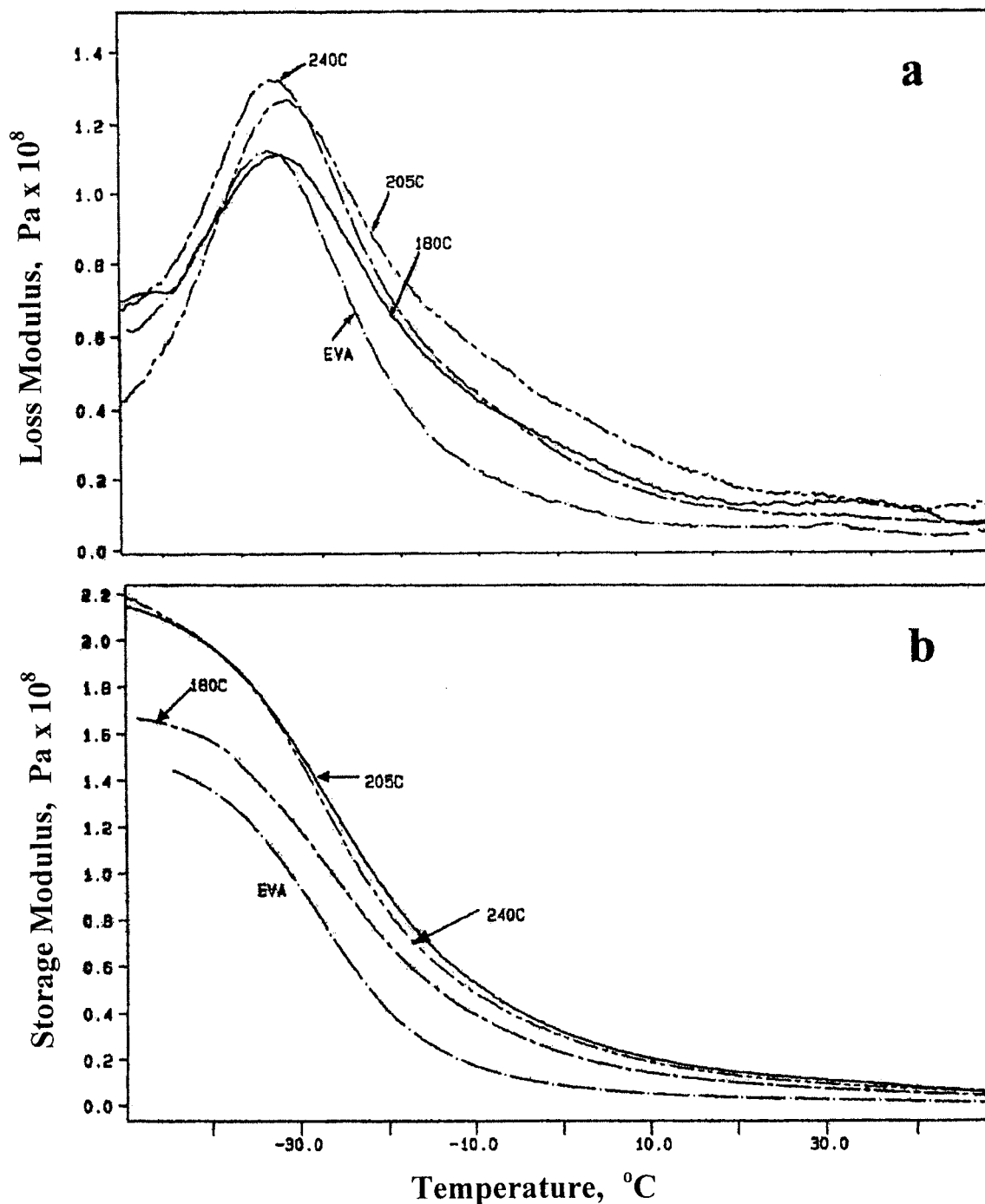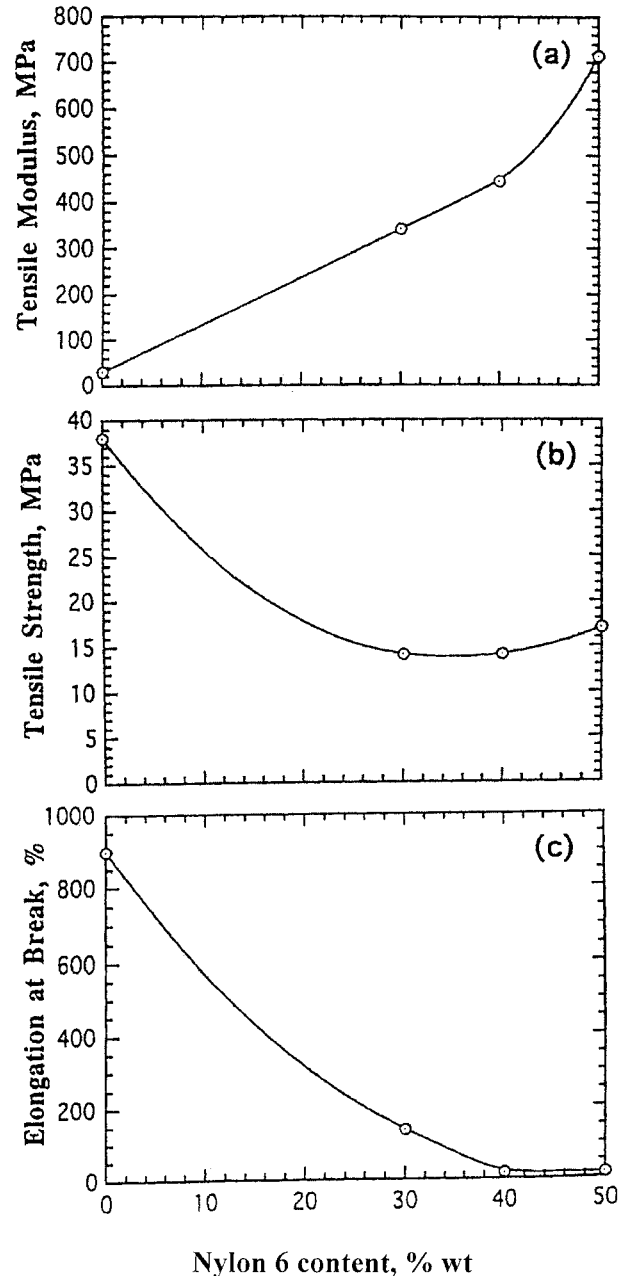


**Figure 4**   The DMTA results of neat EVA and 70EVA/30N6 (Capron) blends for the transverse direction.

unaffected, probably due to the much higher processing temperatures than the EVA melting temperature (~90°C). The capillary rheometer flow curves of the EVA/N6 blends and the neat polymers[21] showed that, for given shear rate and temperature, the apparent viscosity of the blends was lower than that of the N6. The viscosity of the blends seemed to be only slightly temperature



**Figure 5** The tensile properties of injection-molded 70EVA/30N6 blends as a function of the processing temperature. Two procedures were used for the compounding.

a higher viscosity than the N6, but in the higher shear rates range (more relevant to the processing conditions) the viscosity of the two polymers was similar. The viscosity of the Polyram N6, which was measured at the same temperature, was lower than that of the Capron N6 (not shown). The viscosity of the EVA was also measured at the other studied processing temperatures (not shown) and was found to be almost



**Figure 6** The tensile properties of injection-molded EVA/N6 blends as a function of the composition and compounded by injection molding at 205°C.
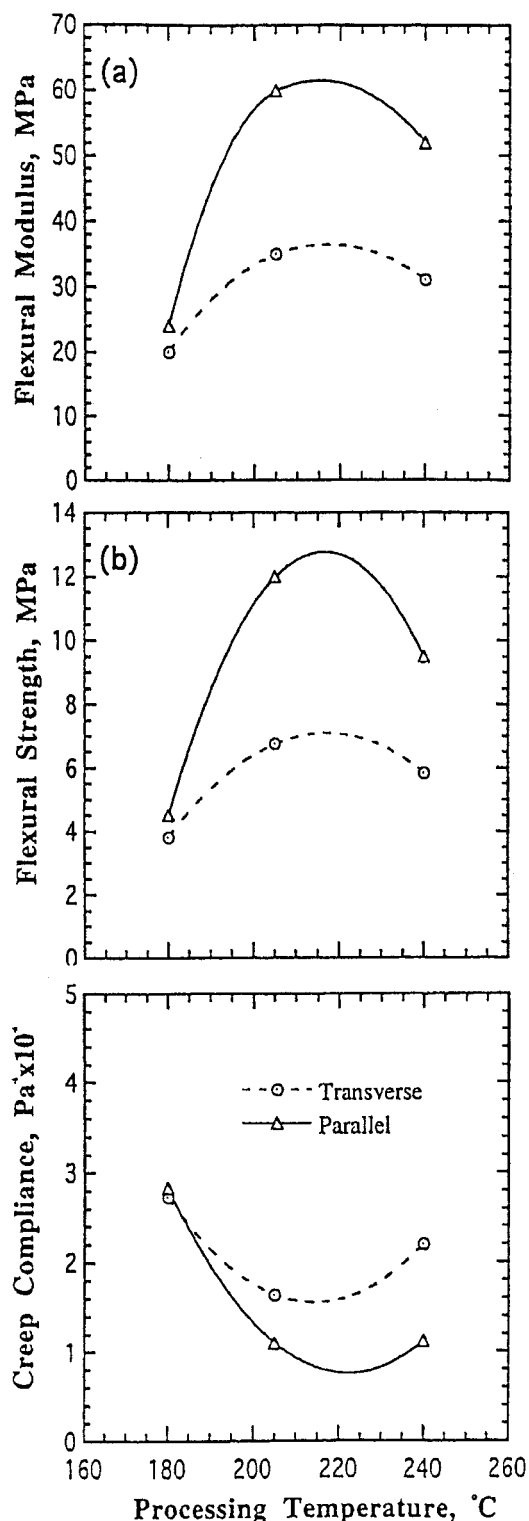
**Figure 7** The mechanical properties in the creep mode in flexure (DMTA) of injection-molded 70EVA/30N6 (Capron) blends as a function of the processing temperature in the transverse and parallel directions.

dependent in the range studied (220–260°C), but Dumoulin et al. reported the common temperature effect for HDPE/N6 blends.[14] The mode and state of dispersion of the minor component in each system could be the reason for this behavior. The extent of deformation of the minor phase depends on its viscosity, relative to the viscosity of a given matrix: the higher the minor phase melt viscosity, the greater is the deformation level obtained.[19]

The melt elasticity play an important role in the phenomenon of die swell, which is well known. The extrudate die swell ratio as a function of the extrusion temperature is depicted in Figure 3. (The die swell was measured on filaments produced through a circular rod die attached to the Brabender twin extruder.) The high die swell values at the intermediate processing temperatures (close to the N6 $T_m$) were caused by axial retraction of the highly elongated N6 fibrils upon exiting the die. At these intermediate processing temperatures the deformation mechanism was that of drawing of a soft solid.[15] Figure 3 is actually important supporting evidence of the concept of compounding–processing at a temperature slightly below the melting peak of the dispersed phase, the focal point of this study.

**DMTA Measurements**

Figure 4 depicts the loss and storage moduli as a function of temperature of the neat EVA and the 70EVA/30N6 blends that were injection molded at different temperatures. Specimens were cut perpendicular to the flow direction. The damping peak of the 70/30 blend occurred at the same temperature as neat EVA [Fig. 4(a)], which were both processed at 180°C; however, the latter was narrower than the peaks of the blends. The damping level of the blends increased with the processing temperature, while their peak shape remained practically unchanged. As expected, the neat EVA exhibited the lowest storage modulus [Fig. 4(b)]. The blends injection molded at 205 and 240°C were similar and had a much higher storage modulus compared to the neat EVA. The blends processed at 180°C showed an intermediate modulus value due to the addition of N6 particles. The higher modulus values of the 205 and 240°C processed blends stemmed from the orientation of and within the N6 phase. The differences decreased with the temperature, becoming insignificant above 30°C, the rubbery state of the blend component.

## Mechanical Properties

The tensile properties of the 70EVA/30N6 injection-molded blends prepared by injection molding or extrusion are shown in Figure 5. The tensile modulus increased with the processing temperature. Of interest were the values obtained for the blend compounded by injection molding, which exhibited an extreme at 210°C. The variation of the tensile modulus with the processing temperature reflected the structures obtained during processing. Blends processed at 210 and 220°C behaved as fiber reinforced composite materials. Oriented fibrillar structures formed along the flow direction (see below) and resulted in the high rigidity values in that direction. The fibrillar structure had already formed in the compounding step; however, because of granulation prior to processing, the fibril orientation along the injection molding direction was not fully preserved after processing. The difference in the tensile properties shown in Figure 5 may be related to the quality of the fibrillar morphology formed by

the two different compounding methods. The tensile strength and elongation at break significantly increased with the processing temperature, exhibiting local maxima at 210°C. Interestingly, the extruded blends had somewhat higher values. For both processing methods the ultimate elongation was significantly higher for the blend processed in the molten state (240°C). The tensile properties of blends injection molded at 205°C as a function of the N6 content are shown in Figure 6. The tensile modulus was remarkably increased with the N6 content, but the tensile strength and elongation at break decreased. At 50 wt % N6 the blend became brittle, exhibiting high rigidity and maintaining a significant strength value. It should be noted that 205°C was the onset temperature of the N6 melting peak. At this processing temperature most of the crystalline phase still existed; however, its mechanical properties were already of a soft, deformable material.

The mechanical properties of the 70EVA/30N6 blends processed by injection molding and studied
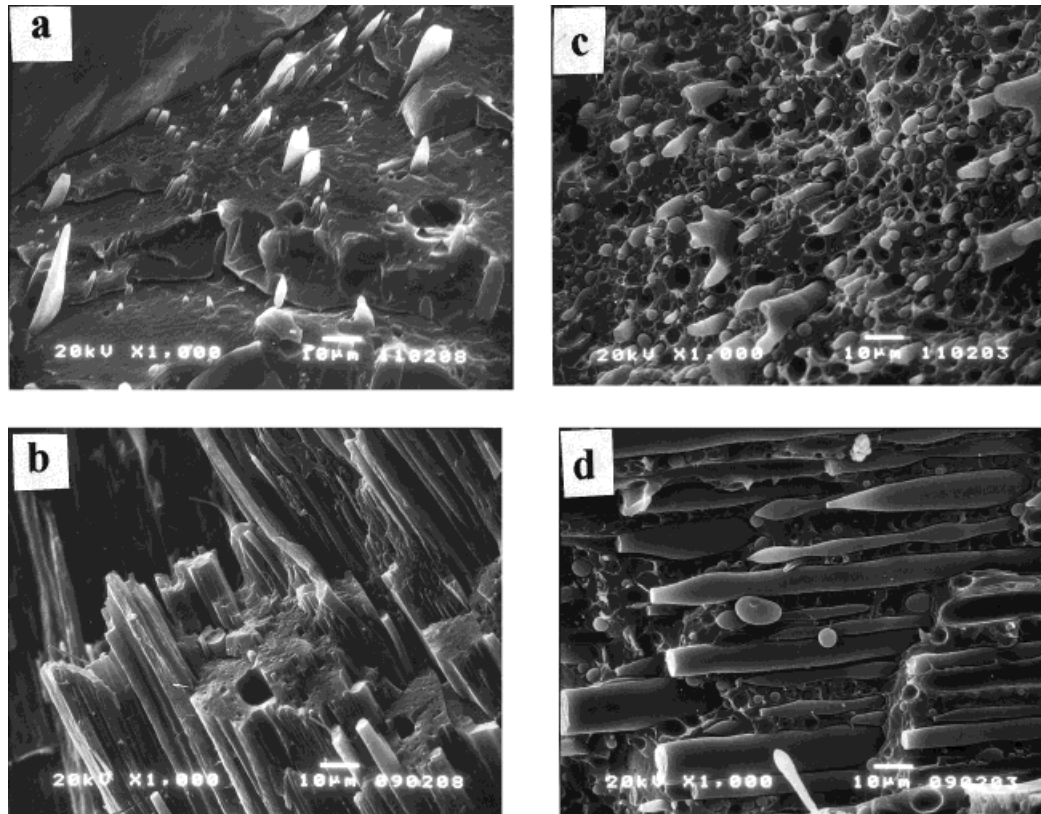


**Figure 8**   SEM micrographs of cryogenically fractured surfaces (fractured at a small angle to the flow direction) of injection-molded specimens of 70EVA/30N6 blends at (a) 190, (b) 210, (c) 220, and (d) 240°C.
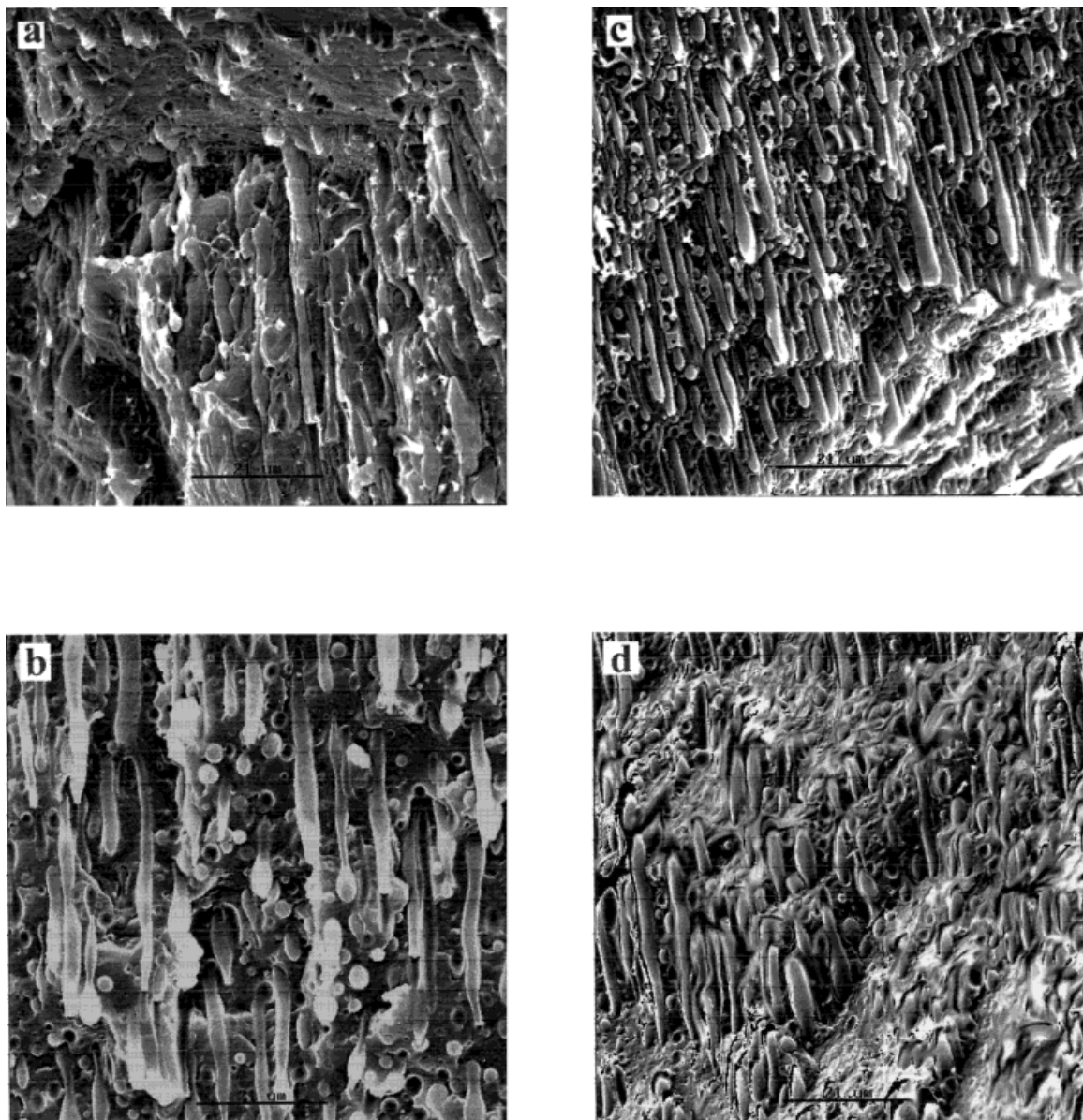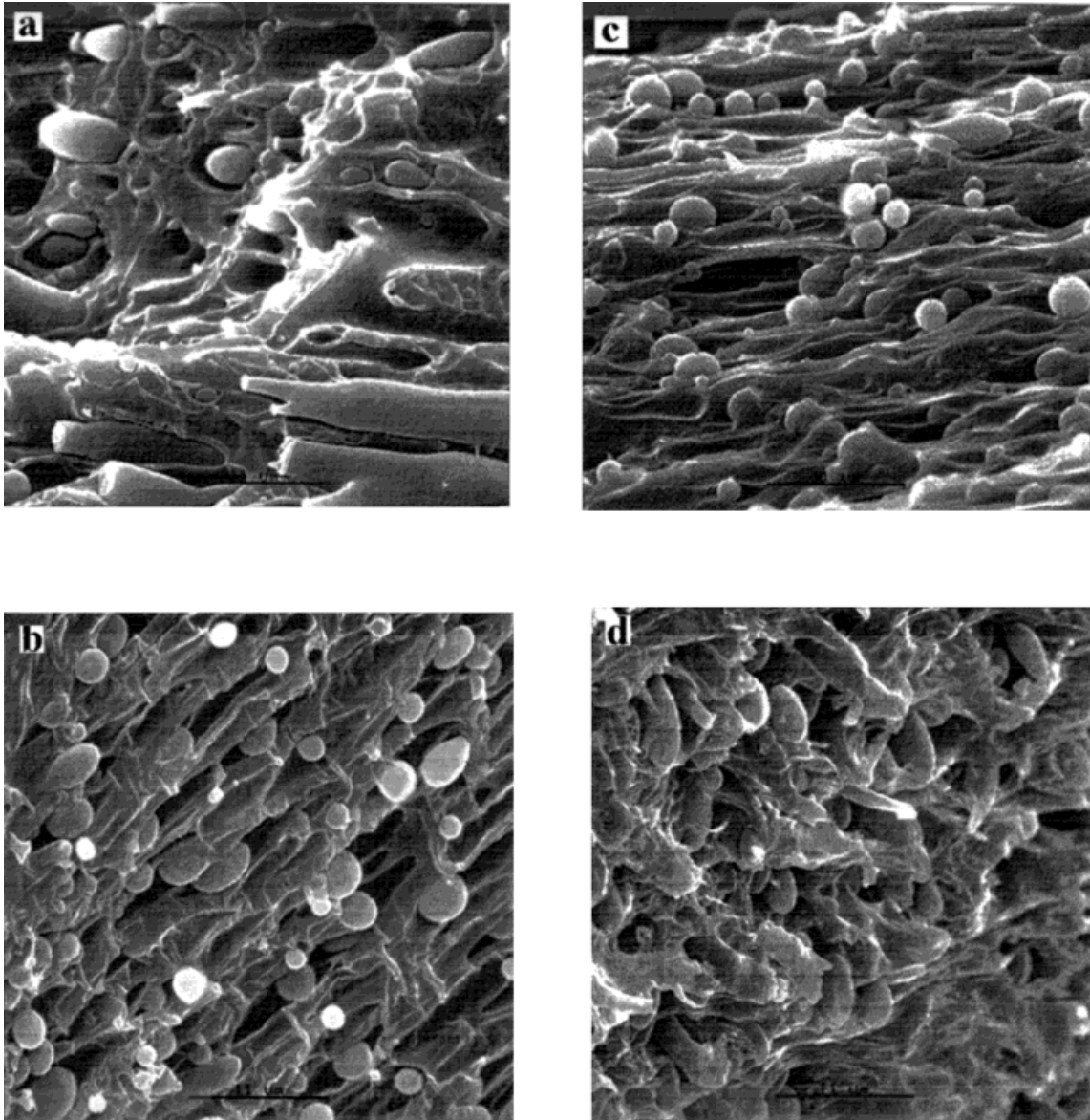
**Figure 9**   SEM micrographs of cryogenically fractured surfaces (fractured at a small angle to the flow direction) of circular extrudates of 70EVA/30N6 blends at (a) 190, (b) 205, (c) 215, and (d) 240°C.

by DMTA are depicted in Figure 7; the flexural strength, flexural modulus, and creep compliance are shown for the different processing temperatures. The DMTA technique requires small specimens ($3 \times 1 \times 20$ mm³), which were cut from the injection-molded dumbbells in parallel and perpendicular directions to the flow. At the intermediate processing temperatures, where the dispersed particle deformation mechanism was that of soft-solid drawing, the flexural modulus and strength showed maximum values. The creep compliance was affected by the processing temperature, attaining a minimum value at the intermediate temperature. The properties as depicted in Figure 7 showed anisotropy in the injection-molded blends, excluding those processed at the low temperature of 180°C. In the latter the dispersed N6 phase indeed acted as a rigid filler. The flexural modulus and strength of the blends processed at the intermediate temperatures was remarkably increased with the N6 content (not shown).

**Figure 10** SEM micrographs of cryogenically fractured surfaces of filaments of 70EVA/30N6 blends drawn up to ~500% extension and extruded at (a) 190, (b) 205, (c) 215, and (d) 240°C.

### Morphology

Figure 8 depicts the core region of the dumbbell-shaped specimens molded at different processing temperatures. Figure 9 shows the structure of the core region of the extruded filaments produced by the Thoret single-screw extruder using a circular rod die. The fibrillar morphology of the dispersed N6 phase was obtained, irrespective of the preparation method used, throughout the entire filament volume rather than within the outer skin region, as commonly observed. With a decreasing

processing temperature the N6 fibrils became smaller in diameter and less regular. When the N6 was fully molten (240°C), the fibril shape reflected deformation of viscous droplets. However, in a partially molten state (210°C), the fibril shape indicated uniform deformation, which is typical of a rubbery material. At processing temperatures below the onset of melting (190°C), the N6 soft particles became highly deformed during processing and formed irregularly shaped elongated particles with a rather wide size distribu-

tion. These particles, because of their low formation temperature, consisted of oriented chains and crystals in addition to their oriented morphology. It was recently reported that EVA/N6 blends prepared at 260°C and injection molded at lower temperatures[15] also showed a fibrillar morphology of the dispersed phase. It was found that the average diameter of the fibrils was comparable to the average size of the original droplets, while their volume was many times larger.[15] The fibrillation process was described as associated with a specific shear-induced coalescence.[15] The present extruded filaments also showed that the morphology had a strong dependence on the processing temperature (Fig. 9). At 190°C no fibrils were formed; instead an oriented layered structure was observed. When the N6 phase was partially or fully molten, fibrils and particles were both formed during extrusion. The fibrils were highly oriented and their irregularity increased with a decreasing processing temperature. The particles were probably the result of fibril rupture. The SEM micrographs of the nitrogen fracture surfaces of extended filaments to ~500% extension are noteworthy (Fig. 10). At a low processing temperature (190°C) the extrusion of the EVA matrix did not show signs of high deformation while some N6 elongated domains produced during processing were seen [Fig. 10(a)]. For the intermediate temperature processed filaments [Fig. 10(b,c)], after rupture in tension, the highly oriented fibrils retracted into spherical domains, leaving elongated cavities in the matrix. The elongated cavities were formed around the N6 fibrils. These results were in agreement with the melt elasticity data shown in Figure 5, where the highly oriented fibrils caused the high die swell. At the high temperature (240°C) the processed filaments showed the expected structure of a blend that was highly stretched (250%); the matrix was also ruptured.

The effect of the viscosity of the N6 dispersed phase on the phase morphology of injection-molded blends was studied using 70EVA/30N6 blends to which a small amount of CB was added. These blends were processed at 210°C, which was at the beginning of the melting peak of N6 (219°C). Uniform, well-arranged fibrillar structures were obtained with the higher melt viscosity Capron N6 [Fig. 11(a)]; the CB particles were distributed very finely throughout the EVA matrix, thus posing difficulty in observing them. For the lower melt viscosity Polyram N6 [Fig. 11(b)] the fibrillar structure was less regular and the CB
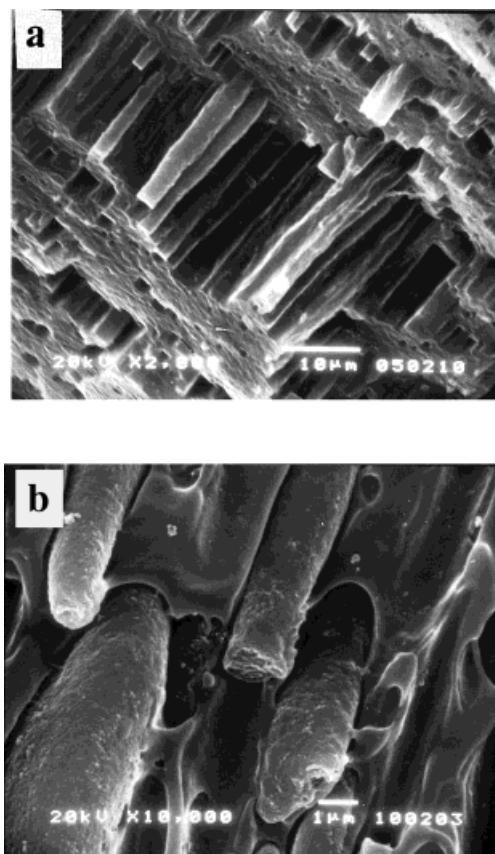
**Figure 11** SEM micrographs of cryogenically fractured surfaces of injection-molded specimens of (a) 70EVA/30N6 (Capron)/2CB blends and (b) 70EVA/30N6 (Capron)/2CB blends molded at 210°C.

particles were located at the surface of the N6 fibrils. The N6 viscosity thus played an important role in the dispersive mixing process: deagglomeration, aggregate fracturing, and particle distribution by flow and flocculation all took place within the matrix. The higher viscosity N6 may have enhanced the deagglomeration and fracturing of the aggregates.

## CONCLUSIONS

Compounding and processing were carried out at the same temperature in a range from slightly below to above the melting temperature of the dispersed phase (N6) and always well above the melting temperature of the matrix (EVA). The results of the study led to the following conclusions:

1. The melt elasticity of the filaments, which was measured by die swell, was maximal

at a temperature slightly below the N6 peak melting temperature, which supported the concept of processing slightly below the $T_{m,\text{N6}}$ of the dispersed phase.

2. A hot soft-solid particle drawing mechanism that was operating during processing at $T < T_{m,\text{N6}}$ caused fibrillation of the N6 particles throughout the bulk of both the moldings and extrudates. The original size of the dispersed phase particles played an important role in the fibrillation process.

3. High modulus anisotropic composite materials with interesting morphological structures and mechanical properties were obtained when processed at $T < T_{m,\text{N6}}$ of the dispersed phase.

## REFERENCES

1. Favis, B. D.; Chalifoux, J. P. Polymer 1988, 29, 1761.
2. Benderly, D.; Siegmann, A. Polym Compos 1996, 17, 343.
3. Min, K.; White, J. L.; Fellers, J. F. Polym Eng Sci 1984, 24, 1327.
4. Alle, N.; Lyngaae-Jorgensen, J. Rheol Acta 1980, 19, 104.
5. Chin, H. B.; Han, C. D. J Rheol 1979, 23, 557.
6. Kamal, M. R.; Garmabi, H.; Hozhabr, S.; Arghyris, L. Polym Eng Sci 1995, 35, 41.
7. Subramanian, P. M. Polym Eng Sci 1985, 25, 483.
8. Subramanian, P. M.; Mehra, V. Polym Eng Sci 1987, 27, 663.
9. Diluccio, R.; Dell, W. U.S. Pat. 416,942, 1983.
10. Van Oene, H. I. Colloid Interface Sci 1972, 48, 448.
11. Elmendorp, J. J. Polym Eng Sci 1986, 26, 34.
12. Gaona-Torres, J.; Gonzalez-Nunez, R.; Favis, B. D. The influence of melt-drawn ratio and composition on drop coalescence in PA6/HDPE blends. Annu Tech Conf—Soc Plast Eng 1997, 55(2), 2597–2601.
13. Gonzalez-Nunez, R.; De Kee, D.; Favis, B. D. Polymer 1996, 37, 4689.
14. Dumoulin, M. M.; Toma, P.; Utracki, L. A. Melt flow polyethylene/polyamide blends; Part I: HDPE/PA-6. Annu Tech Conf—Soc Plast Eng 1985, 43(2), 534–536.
15. Utracki, L. A.; Dumoulin, M. M.; Toma, P. Polym Eng Sci 1986, 26, 34.
16. Min, K.; White, J. L. Polym Eng Sci 1984, 24, 1327.
17. Chapleau, N.; Favis, B. D.; Carreau, P. J. Morphology of polyamide/polyethylene blends under extensional flow: effect of compatibilization. Annu Tech Conf—Soc Plast Eng 1997, 55(2), 1695–1699.
18. Li, X.; Chen, M.; Huang, Y.; Cong, G. Polym Eng Sci 1999, 39, 881.
19. Addonizio, M. L.; D'Orazio, L.; Mancarella, C.; Martuscelli, E.; Casale, A.; Filippi, A. J Mater Sci 1989, 24, 2939.
20. D'Orazio, L.; Mancarella, C.; Martuscelli, E.; Casale, A.; Filippi, A.; Speroni, F. J Mater Sci 1987, 22, 429.
21. D'Orazio, L.; Mancarella, C.; Martuscelli, E.; Casale, A.; Filippi, A.; Speroni, F. J Mater Sci 1986, 21, 989.